# Programmable Payload Release from Transient Polymer Microcapsules Triggered by a Specific Ion Co-Activation Effect

Shijia Tang,<sup>†,‡</sup> Liuyan Tang,<sup>†</sup> Xiaocun Lu,<sup>†,||</sup> Huiying Liu,<sup>†,||</sup> Jeffrey S. Moore<sup>\*,†,‡,||</sup>

†Beckman Institute for Advanced Science and Technology, ‡Department of Materials Science and Engineering, and <sup>||</sup>Department of Chemistry, University of Illinois at Urbana–Champaign, Urbana, Illinois 61801, United States

Supporting Information Placeholder

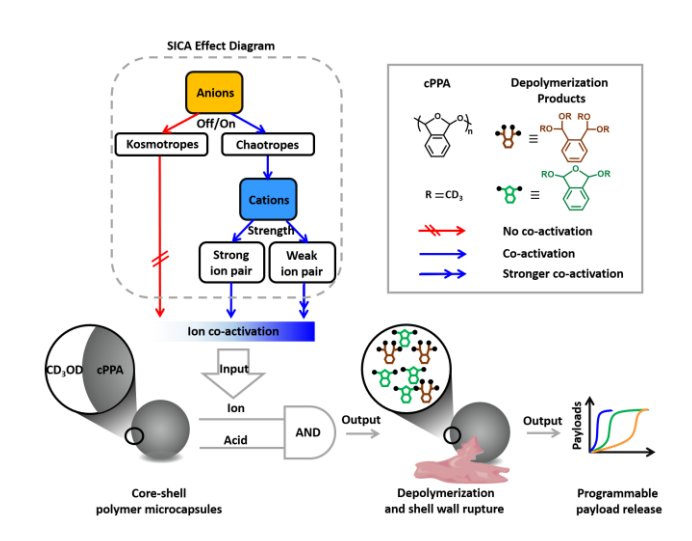
ABSTRACT: Stimuli-responsive materials activated by a pair of molecular or ionic species are of interest in the design of chemical logic gates and signal amplification schemes. There are relatively few materials whose co-activated response has been well-characterized. Here, we demonstrate a specific ion co-activation (SICA) effect at the interfaces of transient polymer solids and liquid solutions. We found that depolymerization of the transient polymer, cyclic poly(phthalaldehyde) (cPPA), exhibited a SICA effect when the cPPA core-shell microcapsules were suspended in ion-containing acidic methanol solutions. Significant acceleration in cPPA depolymerization rate is triggered by the combination of acid and ion co-activators. Intriguingly, the SICA effect is related to the Hofmeister behavior. The SICA effect is primarily determined by anions, and cations exhibit a secondary effect that modulates the coactivation strength. Based on these observations, we developed cPPA programmable microcapsules whose payload release rates depend on the composition and concentration of the salt/acidicmethanol solutions.

In biological systems, homeostasis depends on accurate and autonomous regulation, leading to intricate, feedback-controlled reaction networks. Some feedback controlled mechanisms originate from specific ion-biomolecule interactions that regulate enzyme (de)activation, signal transduction, and cell volume. For example, Ca²+ inhibits lipid recognition by direct binding to the lipid marker phosphatidylinositol 4,5-bisphosphate in plasma membranes, whereas Mg²+ exhibits only a modest inhibition effect. This specific ion-biomolecule interaction is mostly attributed to different ion dehydration energy penalties originally studied by Hofmeister in the 1880s. So far, the specific ion effect has been applied to (bio)catalysis, protein aggregation, since in the specific ion effect has been applied to (bio)catalysis, protein aggregation, since ion effect has been applied to (bio)catalysis, for in the specific colloidal systems stability, since in the specific ion effect has been applied to (bio)catalysis, for in the specific colloidal systems stability, since in the specific ion effect has been applied to (bio)catalysis, for in the specific colloidal systems stability, since in the specific ion effect has been applied to (bio)catalysis, for in the specific colloidal systems stability, since in the specific ion effect has been applied to (bio)catalysis, for in the specific ion effect has been applied to (bio)catalysis, for in the specific ion effect has been applied to (bio)catalysis, for in the specific ion effect has been applied to (bio)catalysis, for in the specific ion effect has been applied to (bio)catalysis, for in the specific ion effect has been applied to (bio)catalysis, for in the specific ion effect has been applied to (bio)catalysis, for in the specific ion effect has been applied to (bio)catalysis, for interaction is not provided to the specific ion effect has been applied to (bio)catalysis, for interaction is not provided to the specific ion effect has been applied to (bio)catalysis, for interaction is not

In contrast, the specific ion effect has been less commonly employed in synthetic materials but has potential in the design of materials with bio-inspired functions. For example, combining a specific ion effect with compartmentalized materials, microcapsules<sup>23</sup> and vascularized composites,<sup>24</sup> may achieve biomimetic functions such as signal transduction and chemical amplification. One strategy involves ion-triggered microcapsules that transduce ion recognition into the release of an encapsulated payload.<sup>25,26</sup> Microcapsules whose shell walls consist of transient polymers are a promising possibility.<sup>27–29</sup> Typically, the transient polymers undergo chain unzipping depolymerization after removing end groups or cleaving

the backbone by stimuli.<sup>28,30</sup> It has been shown that the depolymerization leads to rupture of the microcapsule's shell wall, releasing the payloads with sigmoidal-shaped kinetic profiles.<sup>25</sup> Specific ion effects at the interfaces of transient polymer microcapsules are possible design components for feedback controlled reaction cascades. However, the specific ion effect has not been addressed in previous studies on transient polymers.

Scheme 1. The SICA Effect at the Transient Polymer Microcapsule's Interfaces and Reaction Output.



Cyclic poly(phthalaldehyde) (cPPA) is an acid triggered transient polymer. Acids react with the cPPA polyacetal backbone to initiate a chain unzipping depolymerization. 31,32 cPPA has been previously used as the shell wall materials of acid responsive microcapsules.<sup>29</sup> Depolymerization in mildly acidic solution is slow especially at solid/liquid interfaces such as microcapsule suspensions. Here, we report a specific ion co-activation (SICA) effect at the interfaces of transient polymer solids and liquid solutions, using cPPA core-shell microcapsules suspended in acidic methanol. (Scheme 1). We demonstrate that the SICA effect accelerates cPPA interfacial depolymerization in mildly acidic methanol solutions (Scheme 2), triggering shell wall materials transience and greatly accelerates payload release rates. The ions have no intrinsic effect to trigger cPPA depolymerization, but rather exhibit co-activation behavior with acid to tailor the depolymerization rates depending on the ionic species. The SICA effect is related to the Hofmeister series, and anions are the dominant factor to determine the co-activation effect. Cations modulate the co-activation effect by pairing with anions, where a weaker ion pair result in a stronger co-activation.

# Scheme 2. cPPA Depolymerization in Acidic d<sub>4</sub>-methanol Solutions.<sup>a</sup>

<sup>a</sup> Depolymerization products remained the same regardless of the depolyerization conditions (+/- ions) used in this study.

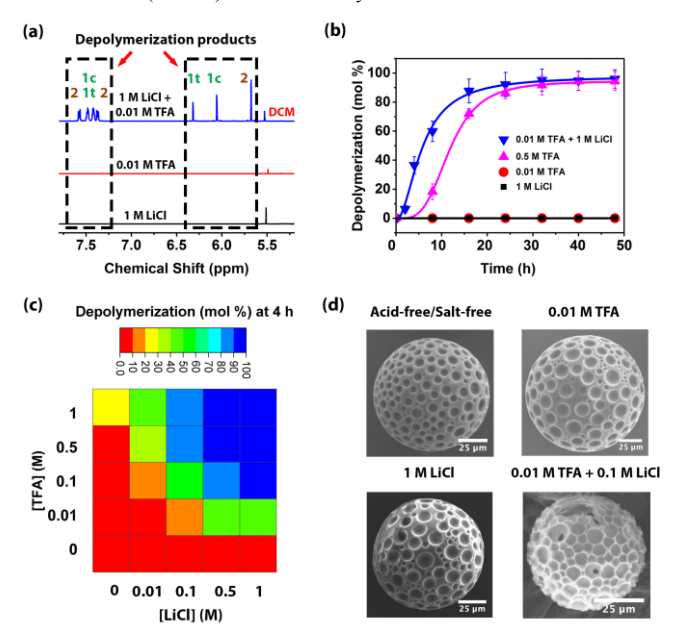


Figure 1. The co-activation effect in LiCl/TFA/CD<sub>3</sub>OD solutions. (a) <sup>1</sup>H NMR spectra of microcapsules suspended in various triggering solutions for 24 h. Dichloromethane (DCM) was the residual solvent from the microcapsule's preparation. (b) Shell wall depolymerization profiles measured by NMR using ethylene glycol as an internal standard. Data plots were fitted to an empirical logarithmic function. (c) Summary of depolymerization mol % at 4 h in varied concentrations of salts and acid solutions. (d) SEM images of microcapsules suspended in various solutions showing the morphology changes after 24 h treatment.

The SICA effect was first discovered and confirmed using LiCl by nuclear magnetic resonance (NMR) spectroscopy and microscopy studies (Scheme 2, Figure 1, S1-S4). We prepared the cPPA microcapsules with a core of jojoba oil and Nile red (for visualization and payload release profile measurements) by a rapid solvent evaporation procedure.<sup>29</sup> The cPPA microcapsules were suspended in  $d_4$ -methanol solutions containing trifluoroacetic acid (TFA), LiCl or both. We chose methanol as the medium because the microcapsules disperse and suspend favorably and this solvent has good solubility for salts compared with other organic solvents. Samples suspended in TFA (0.01 M in CD<sub>3</sub>OD) for 24 h showed no depolymerization (Figure 1 (a), red), because this concentration of TFA was too low to initiate rapid depolymerization. Also, samples suspended in LiCl (1 M in CD<sub>3</sub>OD) showed no depolymerization products (Figure 1(a), black). In great contrast, significant cPPA depolymerization was observed in solutions containing both TFA (0.01 M) and LiCl (1 M) based on the highlighted aromatic

and acetal peaks. The depolymerization products were *trans* (1t) and *cis* (1c) isomers of 1,3-dihydro-1,3-dimethoxyisobenzofuran and 1,2-bis(dimethoxymethyl)benzene (2) as determined by NMR spectroscopy. The products were consistent with a previous report on *o*-PA reacting with methanol. (Scheme 2, S1, Supporting information).<sup>33</sup> The products remained the same in all triggering conditions in this study.

To quantify the depolymerization rates, we tracked the depolymerization products formation over 48 h using ethylene glycol as an internal standard (Figure 1(b)). Fitting the depolymerization profiles to an empirical logarithmic function, we extracted the shell wall depolymerization half-life ( $t_{D50}$ ). In either TFA or LiCl solutions, no depolymerization was observed and no  $t_{D50}$  values were obtained (Figure 1(b), red and black traces).  $t_{D50}$  in TFA (0.01 M) and LiCl (1 M) mixed solution was  $6.0 \pm 0.5$  h (Figure 1(b), blue trace). This  $t_{D50}$  was even shorter than that of microcapsules suspended in 0.5 M TFA solution ( $12.2 \pm 0.3$  h, Figure 1(b), pink trace). The addition of LiCl led to significant acceleration in the depolymerization rates. Notably, however, LiCl by itself had no effect on the depolymerization kinetics over two weeks, confirming that LiCl was a co-activator (Figure S5, S6).

To further demonstrate the co-activation effect and tunable depolymerization rates, we varied the combination of TFA and LiCl concentrations and plotted the depolymerization mol % at 4 h in Figure 1(c). The synergistic trigger (TFA and LiCl) resulted in depolymerization ranging from 12 mol % to more than 90 mol %, and apparently, always led to more depolymerization compared with the individual trigger, TFA or LiCl, of the same concentration. We further verified the co-activation effect in alternative acid solutions, HCl and *p*-toluene sulfonic acid (PTSA) (Figure S7). Similarly, adding LiCl in these acid solutions resulted in accelerated and tunable depolymerization rates.

The morphology changes induced by cPPA shell wall depolymerization were confirmed by SEM and optical microscopy (Figure 1(d), S3, S4). Microcapsules suspended in acid-free/salt-free methanol, TFA (0.01 M), or LiCl (1 M) displayed similar morphologies, identical to the as-synthesized cPPA microcapsule's morphology. They all possessed a golf-ball like surface, attributed to the rapid solvent evaporation during microcapsule's preparation (Figure S1(a)).<sup>29</sup> In contrast, microcapsules suspended in solutions containing both TFA (0.01 M) and LiCl (1 M) exhibited shell wall erosion with visible damage (Figure 1(d), S3(d), S4(d)), resulting from significant shell wall depolymerization.

To demonstrate ion specificity, we investigated the depolymerization profiles for various anions and cations (Figure 2). First, we varied the anions using Li<sup>+</sup> as the counter cation (0.01 M TFA + 1 M lithium salts) (Figure 2(a)). For the kosmotropic anions such as SO<sub>4</sub><sup>2</sup>, F, and OAc-, no co-activation effect was observed, evidenced by their lack of depolymerization mol % at 16 h (0 mol %) compared to that in 0.01 M TFA (salt-free) at 16 h (0 mol %) (Figure 2(a), Figure S11). For chaotropic anions, the depolymerization half-life,  $t_{D50}$ , was  $ClO_4^-$  (4.2 ± 1.0 h) <  $Cl^-$  (6.0 ± 0.5 h) <  $Br^-$  (8.4  $\pm 0.1 \text{ h}$ ) < I<sup>-</sup>  $(8.8 \pm 0.6 \text{ h}) <$  SCN<sup>-</sup>  $(22.9 \pm 2.5 \text{ h}) <$  NO<sub>3</sub><sup>-</sup>  $(25.7 \pm 1.8 \text{ m}) <$  NO<sub>3</sub><sup>-</sup>  $(25.7 \pm$ h), showing distinct co-activation effects (Figure S12). To further validate the anion specificity, an in situ ion exchange experiment was designed (Figure S13). Microcapsules were first suspended in 0.01 M TFA for 24 h (0 mol % depolymerization), followed by adding 0.05 M LiCl to accelerate the depolymerization from 24 to 42 h. At 42 h, 0.05 M AgOAc was added to exchange Cl- to OAcby forming AgCl. The removal of the chaotropic anion Cl<sup>-</sup> slowed down the depolymerization from 42 to 72 h. This abrupt change in the co-activation behavior at the borderline from kosmotropic anions to chaotropic anions is consistent with the Hofmeister effect, that originates from the difference in anion solvation behavior. 12 The desolvation energy penalties of chaotropic anions are much lower than those of kosmotropic anions. Therefore, the interactions

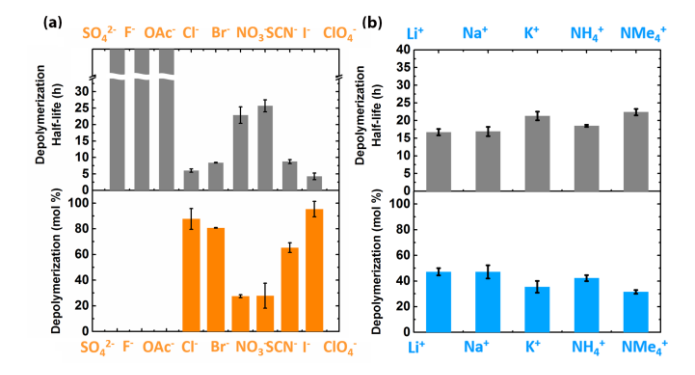


Figure 2. Summary of anion (1 M) and cation (0.02 M) specific effect on depolymerization kinetics for microcapsules suspended in methanol at [TFA] = 0.01 M as represented by depolymerization half-life  $t_{D50}$  and depolymerization mol % at 16 h. (a) Anion specificity in the co-activation (cation = lithium), showing that only chaotropic anions accelerated the depolymerization rates. The  $t_{D50}$  SO $_4^{2-}$ ,  $F^-$ , and OAc $^-$  were marked in break columns because these values exceeded the measuring scale and no depolymerization was observed over 48 h. (b) Cation specificity in the co-activation (anion = chloride), showing a modulating effect on the depolymerization rates.

between chaotropic anions and cPPA are more energetically favorable to co-activate the depolymerization.<sup>35</sup>

Intrigued by the anion specific co-activation effect, we further tested the cation effect using chloride (0.01 M TFA + 0.02 M chloride salts) as the counter anion (Figure 2(b)). A lower concentration was used to allow all ionic compounds soluble in methanol. Li<sup>+</sup>, Na<sup>+</sup>, K<sup>+</sup>, NH<sub>4</sub><sup>+</sup>, NMe<sub>4</sub><sup>+</sup> exhibited modest differences in the co-activation effect, indicating anions are the dominant factor (Figure S14). The dominant role of anions over cations was likely attributed to the stronger interactions of anions with the cPPA/methanol interfaces compared with cations. In general, cations are smaller in size and more solvated compared with anions of similar molar mass; thereby cations are likely to be depleted from a hydrophobic interface while anions are more attracted to it. 10,20,36 The stronger interactions apparently lead to the dominant role of anions in the SICA effect. Cations exhibit a secondary effect that modulates the co-activation inversely to the ion pair strength. A weaker ion pair allows a stronger anion-cPPA interaction and a stronger co-activation (Figure S15, S16).

Also notably, the SICA effect modulated the payload release rates (Figure S17-19). The sigmoidal-shaped payload release profiles were caused by the rupture of the cPPA shell wall, resulting from the chain unzipping depolymerization (Scheme 1). The payload release half-life ( $t_{\rm R50}$ ) correlated with the depolymerization half-life  $t_{\rm D50}$ . A shorter shell wall half-life yielded a faster payload release rate (Figure S19). Because the depolymerization rates were tuned by the SICA effect, the payload release rates were also ion specific.

We further analyzed ion concentration dependence of the SICA effect. In general, we observed a concentration-dependent co-activation effect (Figure 3(a), S20-S22, Table S5, S6). Increasing LiCl concentration from 0.1 M to 1 M reduced the  $t_{D50}$  from  $10.3 \pm 1.5$  h to  $6.0 \pm 0.5$  h. In LiSCN, however, 0.1 M LiSCN ( $t_{D50} = 20.6 \pm 0.5$  h) and 1 M LiSCN ( $t_{D50} = 22.9 \pm 2.5$  h) yielded similar depolymerization rates. We speculated this saturation-type concentration effect in LiSCN was attributed to the affinity of the weakly solvated SCN- to the cPPA interfaces. <sup>11,37</sup> High concentration of SCN- around the cPPA microcapsules was supported by the significantly more negative zeta potential (-42.6 mV) of 1 M LiSCN compared with that of 1 M LiCl (-2.8 mV). Presumably, the highly charged

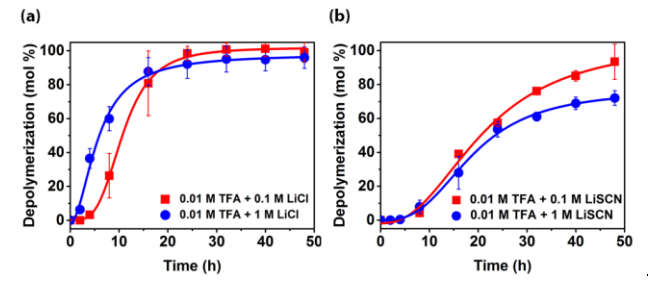


Figure 3. Salt concentration-dependent depolymerization profiles of microcapsules suspended in methanol at [TFA] = 0.01 M with (a) LiCl and (b) LiSCN. Data plots were fitted to an empirical logarithmic function.

surface led to electrostatic screening effect, resulting in a saturation-type of concentration-dependent co-activation for LiSCN. <sup>11,13</sup>

From the ion specificity studies, chaotropic anions were found to be the best co-activators. However, the effect of these anion-cPPA interactions on the depolymerization mechanism is unclear. As anions become less solvated from Cl to ClO<sub>4</sub>, the co-activation effect decreased from Cl<sup>-</sup> to NO<sub>3</sub><sup>-</sup> and increased from SCN<sup>-</sup> to ClO<sub>4</sub><sup>-</sup> (Figure 2(a)), showing a non-monotonic trend. These trends suggested that the SICA effect on the depolymerization kinetics received contributions from several mechanisms. We hypothesize two primary mechanisms contribute to the SICA effect: an ionic effect that stabilizes the depolymerization intermediates (Cl<sup>-</sup> and Br); an electrostatic effect that polarizes the shell wall interfaces (SCN-, I-, ClO<sub>4</sub>). <sup>7,38,39</sup> However, limited studies are available in these area to explain the co-activation effect at the molecular level. Our future work will analyze these mechanisms and incorporate simulation studies to understand the mechanisms of the SICA effect on the depolymerization kinetics.

In summary, we discovered and proved salts as co-activators at the solid/liquid interfaces of transient polymer microcapsules. Variation in anions and cations illustrates that the SICA effect is related to the Hofmeister series, with anions being the dominant factor. This SICA effect enables controlled depolymerization at the cPPA microcapsule's interfaces, which is invaluable for developing iontriggered microcapsules with programmable payload release. We also envision the combination of an acid trigger and an ion co-activator is applicable to design logic-gate materials with controlled (de)activation. We are not aware of other examples using a specific ion effect to modulate the behaviors of transient materials. This co-activation effect is potentially generalizable to other transient polymers, opening new opportunities to build autonomous chemical systems for the next generation of smart materials.

#### **ASSOCIATED CONTENT**

# **Supporting Information**

The Supporting Information is available free of charge on the ACS Publications website. Materials and Methods, control experiments to verify co-activation effect, quantitative NMR, depolymerization profiles, release profiles, model based fitting, NMR spectra (PDF).

## **AUTHOR INFORMATION**

#### **Corresponding Author**

\*ismoore@illinois.edu

## **Author Contributions**

The manuscript was written through contribution of all authors. All authors have given approval to the final version of the manuscript.

#### **ACKNOWLEDGMENT**

The authors would like to acknowledge the funding and technical support from BP through the BP International Centre for Advanced Materials (BP-ICAM) which made this research possible. The authors also acknowledge funding from the Center for Chemical Innovation NSF/CHE-1740597. A portion of this research was carried out in the Frederick Seitz Materials Research Laboratory Center Research Facilities, University of Illinois. S.T. acknowledges the Imaging Technology Group at the Beckman Institute for Advanced Science and Technology for assistance in characterization and Drs. Leilei Yin, Vivian Lau and Xing Jiang for helpful discussion.

## **REFERENCES**

- (1) Warren, J. C.; Stowring, L.; Morales, M. F. *J. Biol. Chem.* **1966**, 241, 309.
- (2) Clapham, D. E. Cell 1995, 131, 1047.
- (3) Clapham, D. E. Cell 2007, 131, 1047.
- (4) Allbritton, N. L., Meyer, T. Cell Calcium 1993, 14, 691.
- (5) Lang, F. J. Am. Coll. Nutr. 2007, 26, 613S.
- (6) Bilkova, E.; Pleskot, R.; Rissanen, S.; Sun, S.; Czogalla, A.; Cwiklik, L.; Róg, T.; Vattulainen, I.; Cremer, P. S.; Jungwirth, P.; Coskun, Ü. J. Am. Chem. Soc. 2017, 139, 4019.
- (7) Lo Nostro, P.; Ninham, B. W. Chem. Rev. 2012, 112, 2286.
- (8) Hofmeister, F. Arch. Exp. Pathol. Pharmakol. 1888, 24, 247.
- (9) Yang, Z. J. Biotechnol. 2009, 144, 12.
- (10) Okur, H. I.; Kherb, J.; Cremer, P. S. J. Am. Chem. Soc. 2013, 135, 5062.
- (11) Heyda, J.; Okur, H. I.; Hladílková, J.; Rembert, K. B.; Hunn, W.; Yang, T.; Dzubiella, J.; Jungwirth, P.; Cremer, P. S. *J. Am. Chem. Soc.* **2017**, *139*, 863.
- (12) Zhang, Y. J.; Furyk, S.; Bergbreiter, D. E.; Cremer, P. S. J. Am. Chem. Soc. 2005, 127, 14505.
- (13) Zhang, Y.; Cremer, P. S. Proc. Natl. Acad. Sci. U. S. A. 2009, 106, 15249.
- (14) Chen, X.; Yang, T.; Kataoka, S.; Cremer, P. S. J. Am. Chem. Soc 2007, 129, 12272.
- (15) Furyk, S.; Zhang, Y.; Ortiz-Acosta, D.; Cremer, P. S.; Bergbreiter, D. E. J. Polym. Sci., Part A Polym. Chem. 2006, 44, 1492
- (16) Zhang, Y.; Furyk, S.; Sagle, L. B.; Cho, Y.; Bergbreiter, D. E.;

- Cremer, P. S. J. Phys. Chem. C. 2007, 111, 8916.
- (17) Kunz, W.; Lo Nostro, P.; Ninham, B. W. W. Curr. Opin. Colloid Interface Sci. 2004, 9, 1.
- (18) Kunz, W. Curr. Opin. Colloid Interface Sci. 2010, 15, 34.
- (19) Gibb, C. L. D.; Oertling, E. E.; Velaga, S.; Gibb, B. C. J. Phys. Chem. B 2015, 119, 5624.
- (20) Gibb, C. L. D.; Gibb, B. C. J. Am. Chem. Soc. 2011, 133, 7344.
- (21) Vrbka, L.; Vondrásek, J.; Jagoda-Cwiklik, B.; Vácha, R.; Jungwirth, P. *Proc. Natl. Acad. Sci. U. S. A.* **2006**, *103*, 15440.
- (22) Fox, J. M.; Kang, K.; Sherman, W.; Heroux, A.; Sastry, G. M.; Baghbanzadeh, M.; Lockett, M. R.; Whitesides, G. M. J. Am. Chem. Soc. 2015, 137, 3859.
- (23) Esser-Kahn, A. P.; Odom, S. A.; Sottos, N. R.; White, S. R.; Moore, J. S. *Macromolecules* **2011**, *44*, 5539.
- (24) White, S. R.; Moore, J. S.; Sottos, N. R.; Krull, B. P.; Santa Cruz, W. A.; Gergely, R. C. R. Science 2014, 344, 620.
- (25) Wong, A. D.; DeWit, M. A.; Gillies, E. R. Adv. Drug. Deliv. Rev. 2012, 64, 1031.
- (26) Bajpai, A. K.; Shukla, S. K.; Bhanu, S.; Kankane, S. *Prog. Polym. Sci.* **2008**, *33*, 1088.
- (27) DiLauro, A. M.; Abbaspourrad, A.; Weitz, D. A.; Phillips, S. T. *Macromolecules* **2013**, *46*, 3309.
- (28) Peterson, G. I.; Larsen, M. B.; Boydston, A. J. *Macromolecules* **2012**, *45*, 7317.
- (29) Tang, S.; Yourdkhani, M.; Casey, C. M. P.; Sottos, N. R.; White,
- S. R.; Moore, J. S. ACS Appl. Mater. Interfaces 2017, 9, 20115.

  DiLauro, A. M.; Robbins, J. S.; Phillips, S. T. Macromolecules 2013, 46, 2963.
- (31) Tsuda, M.; Hata, M.; Nishida, R.; Oikawa, S. J. Polym. Sci., Part A Polym. Chem. 1997, 35, 77.
- (32) Kaitz, J. A.; Diesendruck, C. E.; Moore, J. S. J. Am. Chem. Soc. 2013, 135, 12755.
- (33) Mirsadeghil, S.; Rickborn, B. J. Org. Chem. 1987, 52, 787.
- (34) Hess, B.; Van Der Vegt, N. F. A. Proc. Natl. Acad. Sci. U. S. A. 2009, 106, 13296.
- (35) Marcus, Y. Ion properties; CRC Press, 1997; Vol. 1.
- (36) Lutter, J. C.; Wu, T.; Zhang, Y. J. Phys. Chem. B. **2013**, 117, 10132.
- (37) Wang, L. H.; Zhang, Z. D.; Hong, C. Y.; He, X. H.; You, W.; You, Y. Z. Adv. Mater. (Weiheim. Ger.) 2015, 27, 3202.
- (38) Lund, M.; Vácha, R.; Jongwirth, P. Langmuir 2008, 24, 3387.
- (39) Lund, M.; Vrbka, L.; Jungwirth, P. J. Am. Chem. Soc. 2008, 130, 11582

